

## Article

# Removal of Organic Materials from Mytilus Shells and Their Morphological and Chemical-Physical Characterisation

Alberto Ubaldini <sup>1,\*</sup>, Flavio Cicconi <sup>2</sup>, Sara Calistri <sup>1,3</sup>, Stefano Salvi <sup>2</sup>, Chiara Telloli <sup>1</sup>,  
Giuseppe Marghella <sup>1</sup>, Alessandro Gessi <sup>1</sup>, Stefania Bruni <sup>1</sup>, Naomi Falsini <sup>1</sup> and Antonietta Rizzo <sup>1</sup>

<sup>1</sup> ENEA, Italian National Agency for New Technologies, Energy and Sustainable Economic Development, C.R. Bologna, Via Martiri di Monte Sole 4, 40129 Bologna, Italy; sara.calistri2@unibo.it (S.C.); chiara.telloli@enea.it (C.T.); giuseppe.marghella@enea.it (G.M.); alessandro.gessi@enea.it (A.G.); stefania.bruni@enea.it (S.B.); naomi.falsini@enea.it (N.F.); antonietta.rizzo@enea.it (A.R.)

<sup>2</sup> ENEA, Italian National Agency for New Technologies, Energy and Sustainable Economic Development, C.R. Brasimone, 40032 Camugnano, Italy; flavio.cicconi@enea.it (F.C.); stefano.salvi@enea.it (S.S.)

<sup>3</sup> Department of Pharmacy and Biotechnology, Alma Mater Studiorum, University of Bologna, 40126 Bologna, Italy

\* Correspondence: alberto.ubaldini@enea.it

**Abstract:** A simple and effective method to eliminate the organic component from mussel shells is presented. It is based on the use of hot hydrogen peroxide. Mollusc shells are composite materials made of a calcium carbonate matrix with different polymorphs and numerous biomacromolecules. The described method was used on mussel shells, but it is generalisable and allows the complete removal of these organic components, without altering the inorganic part. Specimens were kept in a H<sub>2</sub>O<sub>2</sub> 40% bath for few hours at 70 °C. The organic layers found on the faces of the shells were peeled away in this way, and biomacromolecules were degraded and removed. Their fragments are soluble in aqueous solution. This easily permits the chemical-physical characterisation and the study of the microstructure. The quality of calcite and aragonite microcrystals of biogenic origin is very high, superior to that of materials of geological or synthetic origin. This may suggest various industrial applications for them. Calcium carbonate is a useful precursor for cements and other building materials, and the one obtained in this way is of excellent quality and high purity.

**Keywords:** chemical treatment; hydrogen peroxide; polymorphs; Raman spectroscopy; microstructure



**Citation:** Ubaldini, A.; Cicconi, F.; Calistri, S.; Salvi, S.; Telloli, C.; Marghella, G.; Gessi, A.; Bruni, S.; Falsini, N.; Rizzo, A. Removal of Organic Materials from Mytilus Shells and Their Morphological and Chemical-Physical Characterisation. *Crystals* **2024**, *14*, 464. <https://doi.org/10.3390/cryst14050464>

Academic Editor: Carlos Rodriguez-Navarro

Received: 19 April 2024

Revised: 4 May 2024

Accepted: 11 May 2024

Published: 16 May 2024



**Copyright:** © 2024 by the authors. Licensee MDPI, Basel, Switzerland. This article is an open access article distributed under the terms and conditions of the Creative Commons Attribution (CC BY) license (<https://creativecommons.org/licenses/by/4.0/>).

## 1. Introduction

Inorganic materials are used by living organisms in an innumerable number of cases and for the most diverse purposes, including uses such as protection, defence, attack, and structures for resistance to loads and mechanical stresses. The mineralised component of vertebrate bones consists mainly of calcium phosphates in the form of apatite and hydroxyapatite [1]. Many marine invertebrates especially, but not only, including molluscs [2], brachiopods [3], and corals [4], use carbonates to build the hard parts of their body, including shells and corallites. Diatoms create their shells, called frustules, using silica (SiO<sub>2</sub>) [5]. Similar structures are observed in Radiolaria [6], with the significant exception of the *Acantharea* group, whose shell is made up of strontium sulphate (SrSO<sub>4</sub>, celestine) [7]. Sponge spicules (the rigid, structural elements in their endoskeleton) are made by calcium carbonate or silica, depending on the species [8]. Crystals based on magnetite are found in the beaks and heads of migratory birds [9], and a high concentration of zinc and manganese are found in scorpions' stings [10] and in the mouthparts of some insects [11]. To achieve the intended purpose of their function, these inorganic materials are organised and structured at the microscopic and sometimes even sub-microscopic level with absolute precision, due to the driving force of evolution rules. Evolution, in fact, selects organisms over time that are more efficiently able to exploit the materials available in their

environment and that can create the best structures for their survival. These examples show how inorganic materials are exploited by living organisms, and in turn they can become useful starting materials for human purposes and industrial activities. Among others, the materials produced by molluscs appear to be the most potentially useful, and they are also produced in large quantities and therefore are easy to use. Many molluscs, as they are soft-bodied animals, have evolved a complex strategy for maintaining and protecting their soft tissues, which relies on the elaboration of an external calcified rigid structure, the so-called shells. The fabrication of the shells by these animals is a very complex set of processes [12]. They require extremely specialised cells, the biomineralised materials can be often very far from the thermodynamical equilibrium, and their shape and morphology are complex and hierarchically organised.

Although the methods of shell biosynthesis among the many different classes of molluscs can be even very different, they have also some general and common features. In practically all cases, the shells are made of calcium carbonate (the gasteropod *Chrysomallon squamiferum*, a species of snail living on deep-sea hydrothermal vent, has a complex shell wherein most of the external layer is made by iron sulphides, especially pyrite ( $\text{FeS}_2$ ) and greigite ( $\text{Fe}_3\text{S}_4$ ) [13]).

Sometimes, these biomineralised inorganic materials have different physical and chemical properties compared to their counterparts of geological origin or that have been synthesised in the laboratory using traditional chemical methods.

For instance, aragonite, one of the calcium carbonate polymorphs, is metastable at room conditions, but it does not transform into the more stable calcite for kinetic reasons; however a phase transition occurs when it is heated. It is interesting to note that in some cases for samples of biological origin, it has been reported [14,15] that this transition temperature can be even 80–100 °C lower (i.e., in the range between 250–380 °C) than the same transition temperature for the mineral that is 480–500 °C [16], also because of a different water content.

The nacre is the iridescent inner shell layer of some molluscs [17]. It is composed of 95 wt% aragonite and 5 wt% organic materials. Because of the presence of this small quantity of organic molecules and polymers and its microstructure, the nacre has strength and toughness 20–30 times higher than that of normal aragonite [18]. Indeed, calcium carbonate of biological origin can also often be found in an amorphous state, something that is very rare in geological or synthetic samples [19]. This may be due to small differences between the same geological or synthetic materials and those of biological origin, such as the presence of specific secondary elements, different contents of crystallisation water, or different degrees of crystallinity or amorphous components, or it possibly can be due to the micro/nanostructure. It should also be kept in mind that inorganic components are often part of very complex composite materials, where organic components also play an important role. In the case of shells, there are proteins, carotenoids, polysaccharides, and other complex organic components that are used by the living animal for growth and to precisely hold together the present microcrystals.

Shells, moreover, are important not only from a biological point of view and for their inherent beauty and charm, but also due to many other characteristics. They are useful bioindicators to monitor the state of natural environments; recently, shells produced as waste from the food industry have been indicated as a valuable material for the production of building materials, possibly even replacing traditional cements. In fact, these consume a large amount of limestone, but the carbonates derived from the shells of molluscs have properties very comparable to it and a much lower environmental impact in terms of carbon dioxide released.

This means, incidentally, that it is of great importance to know in depth all the mechanical, (micro) structural, and thermodynamic properties of their organic and inorganic components. Deepening the knowledge of intrinsic features and morphological aspects of the inorganic part of shells would be important for these characterisations.

However, although it is the prevalent one in terms of mass and volume, the organic components are always present, and they would play a role in any measurement and in the control of properties. It is therefore interesting to identify chemical or physical methods to separate the two components. While it is relatively easy to eliminate the inorganic part, for example by means of an acid bath, it is more complicated to do the opposite. This can be achieved by, for example, immersing the shells in concentrated sodium hypochlorite or ammonium thioglycolate solutions for sufficiently long times [20]. Diluted sodium hypochlorite is useful for removing deposits of algae or bacteria or possibly encrustations; when it is more concentrated, it can attack organic parts and layers of cellular origin, and a partial whitening is achieved. However, the colour of the most external layer on a shell, called periostracum, which is very rich in organic molecules, can be often preserved in this way, indicating that the removal of organic components is partial. Sodium hypochlorite is also used for achieving a fast chitin extraction from the shells of crab, crayfish, and shrimp [21], but, in this case, the extraction of the organic component is more important than the preservation of the starting sample.

Another possibility to whiten shells is to use hydrogen peroxide. It has been reported to be very efficient for this purpose [22–25]. Furthermore, hydrogen peroxide solution has the great advantage of being much less harmful to the environment than the agents mentioned previously, being the by-products essentially only oxygen and water vapour. Whitening was achieved by attacks with peroxide solutions at different concentrations for long periods of time of 24 h or more.

In this work, the action of removing organic components was achieved using solutions at rather high concentrations (40%  $m/v$ ) at higher temperatures. The result was achieved within a few hours, which in itself is interesting for possible applications, because it makes the process attractive from an industrial point of view. It is interesting to observe that by using these conditions, it is also possible to remove the organic molecules that are present inside the shells and not just those present on the surfaces, which is more difficult not always achieved using milder conditions.

At the end of the process, only the inorganic part remains.

This work also aims to present a chemical-physical characterisation of the samples before and after treatment and the evolution as a function of time.

Some *Mytilus* shells have been studied, as this genus is among those with the greatest nutritional importance and one of the greatest geographic distributions, being cosmopolitan. Therefore, it can be considered emblematic for the study of the inorganic components. The properties depend on the structure; the different parts of the shells can have different ratios between calcite and aragonite, and their crystals can have different morphologies. Investigations on some specimens were carried out using characterisation techniques, such as Raman spectroscopy with an optical Raman microscope, X-ray diffraction, scanning electron microscopy (SEM-EDX), and ICP mass spectrometry, which have also been used to determine the presence and nature of trace secondary elements, which can be useful markers.

## 2. Experimental Section

### 2.1. Materials and Methods

*Mytilus* is a cosmopolitan genus of marine bivalve mollusc in the family *Mytilidae*. They have a shell about 5–10 centimetres long, depending on the species, with an elongated oval shape consisting of a right and left half of the shell (valves), which are held together with an elastic lock strap (ligament).

The specimens studied belong to the species *M. Chilensis* (Hupè, 1859) [26], a species widespread on the coasts of South America, being a subject of intensive aquaculture production.

In order to separate the organic part from the inorganic component, the fresh shells were immersed in a 40% ( $m/v$ ) aqueous solution of hydrogen peroxide (Sigma Aldrich, St. Louis, MO, USA) for times ranging from 5 min to 5 h, in order to study the kinetics of the process. The treatments were performed at different temperatures, but the results

described here were carried out at 70 °C. At the end of this process, the colour of the shells changes, and there is an average weight variation of 3–5%. This variation was determined measuring the weight of at least five specimens, at fixed intervals, in order to minimise random effects that could occur on a single sample. Before weight measurement, the samples were carefully dried in an oven.

Highly concentrated hydrogen peroxide is not so stable and tends to decompose over time. For this reason, fresh batches were used as often as possible and were kept in freezer at −18 °C. Under these conditions, it is considered stable, at least for weeks or more.

## 2.2. Instrumental Analysis

Raman spectra of the compounds and mixtures were acquired, at room temperature, by a BWTEK i-Raman plus spectrometer (B&W Tek, Plainsboro, NJ, USA) equipped with a 785 nm laser in the range of 100–3500  $\text{cm}^{-1}$  with a spectral resolution of 2  $\text{cm}^{-1}$ . The measurement parameters, such as acquisition time, number of repetitions, and laser power, were selected for each sample in order to maximise the signal-to-noise ratio. The standard acquisition, however, was 20 repetitions of 10 s each. This instrument has a maximal power of 350 mW, but in most cases, only 10% of it was used. For each spectrum, a reference acquisition was previously carried out with the same parameters to subtract the instrumental background.

X-ray powder diffraction (XRPD) investigations were performed to determine the crystalline phases, using a Philips X'Pert PRO 3040/60 diffractometer (Philips, Amsterdam, The Netherlands) operating at 40 kV, 40 mA, with Bragg–Brentano geometry, equipped with a Cu K $\alpha$  source (1.54178 Å), Ni filtered, and with a curved graphite monochromator. PANalytical High Score software (version 4.1) was used for data elaboration. The XRD acquisitions were performed using these parameters: start position: 10.0125° [2 $\theta$ ]; end position: 99.9875° [2 $\theta$ ]; step size: 0.0250°; scan step time: 6.0000 s, scan type: continuous.

The characterisation, morphology, and composition of the samples were performed by scanning electron microscopy (SEM-FEI Inspect-S, FEI Company Hillsboro, OR, USA), coupled with energy dispersive X-ray spectroscopy (EDX, Oxford Xplore, Oxford Instruments plc, Abingdon, UK). Observations were carried out at different magnifications using both secondary electrons and backscattered electrons detectors at 10 mm working distance, with energy ranging from 10 to 20 KV. The elemental analysis was carried out in the most significant areas of the samples. Data were processed by the software Oxford AZtec One (AZtecLive 6.1 platform).

A triple quadrupole inductively coupled plasma mass spectrometer (ICP-MS-QQQ, 8800 model, Agilent Technologies, Santa Clara, CA, USA) equipped with two quadrupoles, one (Q1) before and one (Q2) after the octupole reaction system (ORS3), installed in a dedicated Clean Room ISO Class 6 (ISO 14644-1 Clean room [27]) with controlled pressure, temperature, and humidity was used for trace analysis of the secondary elements. Quality control standards (QCs) were added in the batch of analysis in order to control the accuracy of the analytical method. The collision cell in Helium Mode (MS/MS) configuration ensures the removal of any spectroscopic interferences caused by atomic or molecular ions that have the same mass-to-charge as analytes of interest.

The shells samples were finely grounded with a laboratory blender, and 0.50 g of grounded shells were mixed in a solution with HNO<sub>3</sub> and H<sub>2</sub>O<sub>2</sub>. TraceSELECT<sup>®</sup> grade 69% HNO<sub>3</sub> was used. High-purity de-ionised water (resistivity 18.2 M $\Omega$   $\text{cm}^{-1}$ ) was obtained from a Milli-Q Advantage A10 water purification system (Millipore, Bedford, MA, USA) for the dilutions. The samples were digested with a microwave digestion system, Speedwave Four model (Berghof, Germany), equipped with temperature and pressure control in PTFE vessels using 4 mL of nitric acid, 3 mL of hydrogen peroxide, and 13 mL of high purity de-ionised water. Complete dissolution was achieved keeping the pressure constant at 30 bar, while the temperature was linearly increased in 5 min from room condition to 200 °C and then maintained for 10 min. After the digestion, the acid mixture was left to cool at room temperature, and after that, it was quantitatively transferred into plastic vials (Falcon<sup>®</sup>

50 mL Polypropylene Conical Tubes, BD Biosciences, Cowley, UK), previously cleaned with nitric solution, and made up to a final volume of 50 mL with high purity de-ionised water.

The multi-element standard solution IV-ICPMS-71 A (10 µg/mL) and the Rare Earth Elements standard solution CCS-1 (100 µg/mL) supplied by Inorganic Ventures (Christiansburg, VA, USA) were used for calibration. The calibration curve was obtained with seven concentration points in the ppb range: 0, 1, 5, 10, 50, 100, and 200 ppb.

Limit of detection (LOD) and limit of quantification (LOQ) were estimated, respectively, as three and ten times the standard deviation ( $\sigma$ ) of 10 consecutive measurements of the reagent blanks according to EURACHEM recommendation.

### 3. Results and Discussion

A bivalve shell is composed of two hinged parts called valves; they are, when the animal is alive, joined by a ligament, a kind of fibrous connective tissue.

A mollusc shell is formed, repaired, and maintained by a part of the anatomy called the mantle. The shells are made up of three layers [28]: the top layer of organic material (periostracum); the middle thick layer of lime (ostracum); and the innermost, silver-white, shiny mother-of-pearl layer (hypostracum). During the animal's life, the shells grow from one side, called the beak, while the raised area around it is known as the umbo. This region is therefore the oldest and the thickest of the valve, while the opposite end is younger and thinner.

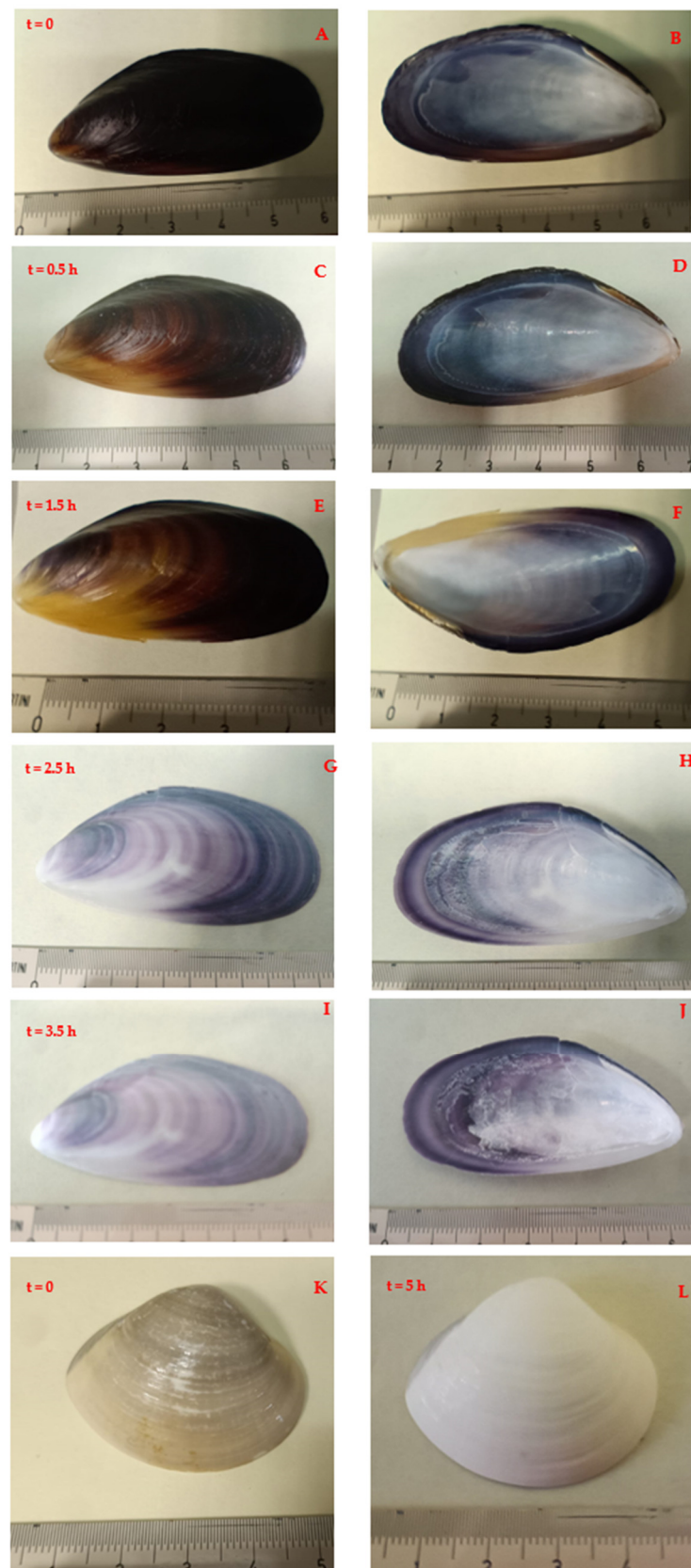
Despite the fact that each species of bivalve has its own peculiarities and the compositions of both the organic and inorganic parts can vary from one case to another, many characteristics of the shells of the genus *Mytilus* could be seen as representative of the entire class of bivalves. In particular, the response to the very oxidising conditions used in this work seems to be general, even shells of molluscs belonging to other classes of this phylum behave in similar way suggesting a much wider field of application of the method.

Figure 1 shows the evolution (in time  $t$ ) of a shell kept in the peroxide bath for a few hours, starting from its initial state:  $t = 0$  (Figure 1A,B). During the process, many small bubbles, of oxygen and water vapour, form on the surfaces of shells.

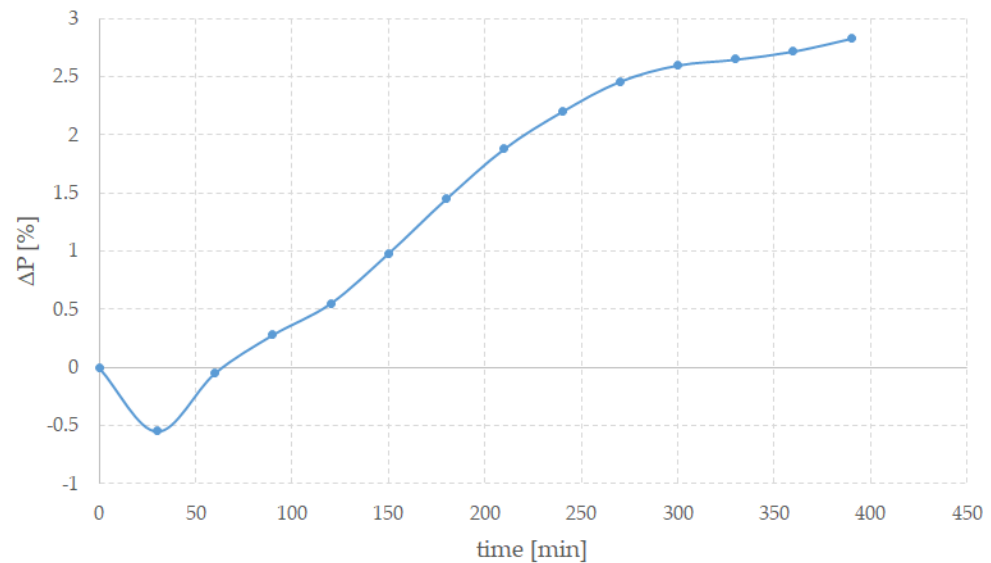
The temperature has a role in the rate of transformation, as the higher it is, the faster the process. However, to avoid any other possible secondary process, the reaction was carried out at 70 °C. It is worth noting that concentrated solutions of hydrogen peroxide are weakly acid [29]. Thus, it may be possible that too much aggressive conditions lead to partial dissolution of the inorganic components too. Very thin sheets, mostly from the inner face, i.e., from the nacreous layer, can detach, very likely because of the mechanical action of bubbles. Valves kept only in hot distilled water do not change in appearance, colour, or weight. Depending on the specimen, some dark lines are still evident in on the valves, even if in some cases white colour is more uniform.

Figure 1K shows an untreated clam shell, while Figure 1L shows the same specimen treated with the same procedure for 5 h. Whitening is also evident in this case, indicating that the method is completely generalisable to other samples, except for a possible different duration of treatment.

At the end of the process, morphology of the shells does not change, while their colour undergoes to a systematic evolution and a small weight loss is observed. After few hours of treatment, shells are white in area of beak and bluish with an almost metallic lustre on the opposite side. Figure 2 shows the trend of the weight variation, averaged over five different samples, and expressed as  $\Delta P = (P_0 - P_t)/P_0 \times 100$ , where  $P_0$  is the initial weight and  $P_t$  is the weight at time  $t$ . Before each measurement, the shells were carefully dried in an oven to eliminate absorbed water.



**Figure 1.** Evolution in time (t) of the appearance of Mytilus valves kept in hydrogen peroxide for different times ((A,C,E,G,I) external face; (B,D,F,H,J) inner face), and a clam valve before the treatment (K) and after 5 h (L).



**Figure 2.** Weight variation  $\Delta P$  (%) for shells kept in hydrogen peroxide bath as a function of time expressed in minutes (min).

It is interesting to note that the weight increased in the early stages of the process (i.e.,  $\Delta P$  is negative), suggesting that initially an absorption of water and, possibly, peroxide inside and on the surface of the shells occurred. After about an hour, the weight decreased monotonically. After about 2 h of treatment, the periostracum and the layer on the inner face began to peel away from the shells in small shreds, revealing the underlying structure and growth lines. This detachment did not occur uniformly across the entire surface of the valve, but preferentially from the edges and from the beak area, i.e., where the layer rich in organic compounds is thinner. Eventually, periostracum completely detached in the form of a thin yellow/brown veil. Eventually the valves were whiter, even if some dark lines were still present. These features could depend on the specific specimen. It should be kept in mind that the composition of valves depends on many factors, starting on the environment where the animal lived. Secondary elements can be absorbed from the marine waters. Parameters, such as temperature, salinity, and water hardness, can play a role in the formation of the shells. Both the living body of a bivalve and its shell are bioindicators of quality of the environment, the presence of any pollution, and the presence of various substances [30].

SEM-EDX analysis showed that the shells were composed of practically pure calcium carbonate, without the evident presence of other elements, at least with concentrations above the sensitivity of this type of measurement, i.e., about 1% or less. Figure 3 shows a typical EDX spectrum of a mussel specimen, and only the peaks due to calcium, carbon, and oxygen were evident, highlighting its remarkable chemical purity.

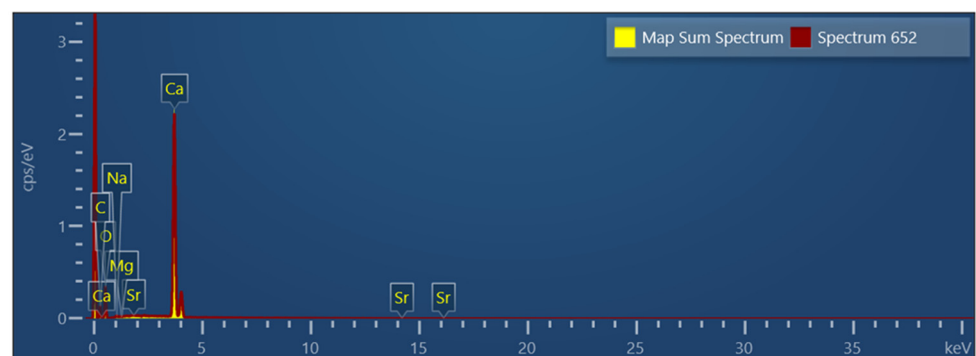


**Figure 3.** EDX spectrum of a *Mytilus* specimen.

Some specimens were also analysed with ICP-MS-QQQ. Table 1 shows the results obtained. RSD (relative standard deviation) for all measurements were below 5%.

**Table 1.** Mean secondary element concentration in the shells, expressed in ppm.

Element	Concentration (ppm)
Sr	83.392
Mg	75.761
K	2.494
Al	1.479
Fe	1.030
Cr	0.125
Mn	0.333
Co	0.996
Ni	0.873
Cu	0.545
Zn	0.423
Ba	0.186
Pb	0.172
U	$1.86 \times 10^{-3}$

Despite the fact that the concentrations of a given element could be different, depending on the environmental conditions in which the animal lived, all these elements, with the only exception of strontium and magnesium, and in particular the heavy metals, were present in rather low concentrations, and this is very important for a possible use of these shells for industrial applications. Heavy metals incorporated into the shell can provide a record of environmental contamination or pollution. Strontium and magnesium, due to their characteristics and chemical similarity, can replace calcium in calcium carbonate, so it should not be surprising that these elements have a higher concentration than the others. It is worth remembering that natural mineral dolomite is a solid solution of calcium and magnesium carbonates, with an ideal ratio between them equal to 1:1 [31].

Chemically, calcium carbonate can be found in different polymorphs: calcite, which is most stable at room temperature and pressure, which crystallises in the hexagonal system; aragonite, which is the densest form; and the hexagonal vaterite, which is less common both in samples of geological origin and in samples of biological nature. Figure 4 shows their crystalline structures.

In a sample of biological origin, all these polymorphs can be found, even if calcite and aragonite are by far the most common, whereas vaterite is rare. Oyster shells are made almost completely by calcite, but in those of other species, both calcite and aragonite are present in different ratios in different points.

These polymorphs have different properties, including mechanical ones, and animals preferentially grow microcrystals of one or the other polymorph based on the functional needs of their shell. For example, where mechanical stresses are concentrated, aragonite is more often found, because it is harder, while in other parts of the shells, a prevalence of calcite is found. These microcrystals are normally organised into complex and ordered structures to better serve the purposes of the shells. In the case of *Mytilus* species, shells grow simultaneously in two directions: the shell grows longer with layers of calcite being added on at the growing edge, and it also thickens, adding layers of aragonite internally [12].

Micro-Raman spectroscopy is a powerful tool for carrying out point-by-point compositional analyses and identifying the present phases. Raman spectra of some points of a valve of an untreated specimen, sampled on both the external and internal surfaces and on the section as well, are shown in Figures 5A and 4B,C, respectively. The points, chosen randomly in such a way as to fully present the characteristics of the shell, represent areas where Raman spectra have been acquired which are then reported in the following figures. The external face appears bluish-dark grey with not very noticeable growth lines; on the contrary, the inner face is mother-of-pearl almost everywhere because of the presence of

the so called nacre, even if on the extremity it is darker, and a rather dark area where the posterior adductor muscle of the animal was attached is easily recognisable (zone number 10); the section, not constant in thickness in all its parts, is instead whitish-yellowish.

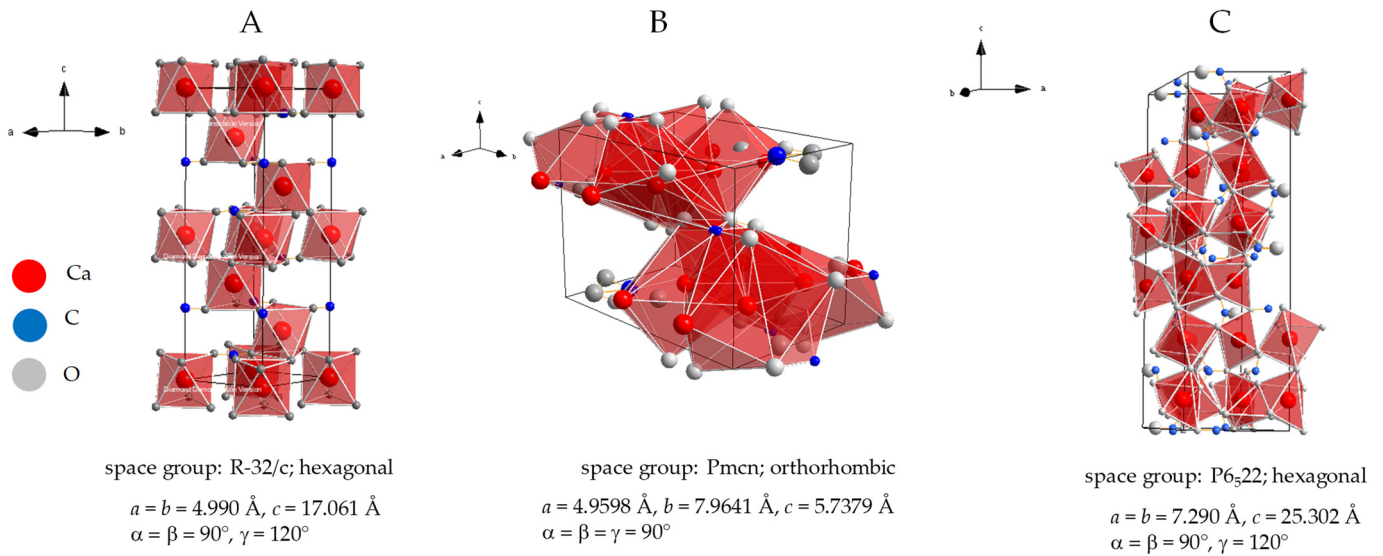


**Figure 4.** Crystal structure of three calcium carbonate polymorphs: calcite (A), aragonite (B), and vaterite (C). Polyhedra represent the oxygen coordination around calcium atoms, that is, octahedral in the case of calcite and more complex for the other two polymorphs: calcium is surrounded by eight oxygen atoms in total, distributed in two non-equivalent positions in vaterite and by nine oxygen atoms in total, distributed in five non-equivalent positions in aragonite. Cell parameters and space group were taken from [32] for calcite, from [33] for aragonite, and from [34] for vaterite. Diamond version 3.2k software was used to draw the crystal structures.

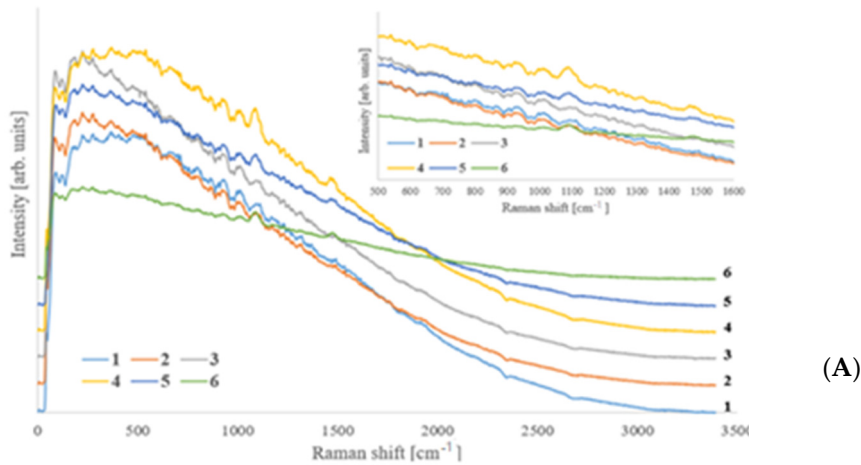


**Figure 5.** Cont.

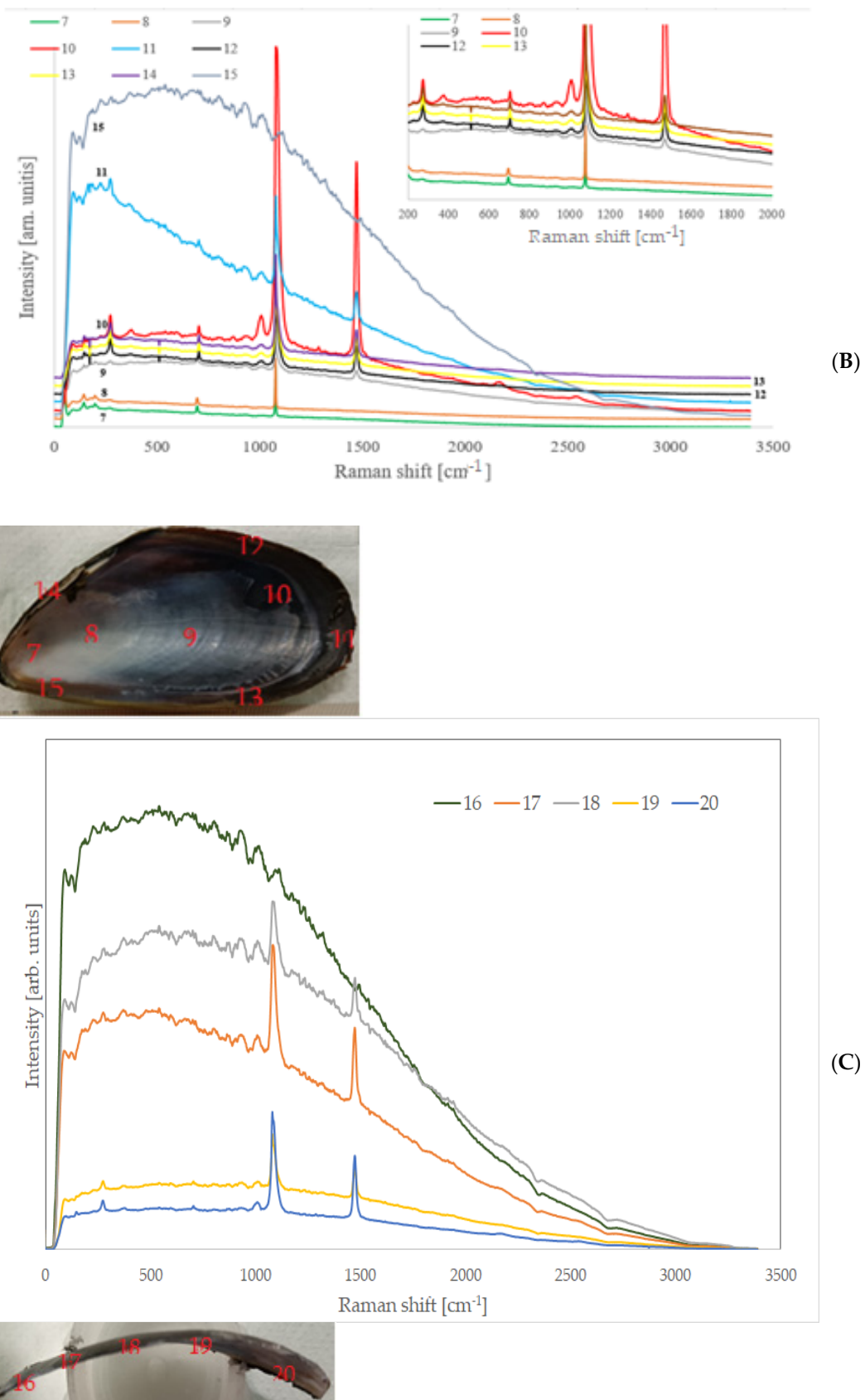


**Figure 5.** Raman spectra of different points on the external face (A), internal face (B), and section (C) of an untreated shell, as it is possible to see in the insets.

Due to the different nature and chemical-physical characteristics of the two faces, the acquisitions of the spectra were optimised in terms of laser power, duration of a single acquisition, and number of repetitions, specifically for each of them.

Raman spectra of the external face are characterised by predominant fluorescence, and different bands were present, as it can be seen in the inset showing the spectra in the characteristic zone between 500 and 1600  $\text{cm}^{-1}$ . It is difficult to attribute these bands to specific chemical components, and even the inorganic part cannot be recognised immediately in any point because the characteristic peaks of calcite and aragonite fall in areas of the spectrum where many signals of different origin are present. In general, the same signals, regardless with their relative intensity and the fluorescence intensity, were present in all the spectra. This means that the same components were present, even if possibly in relative quantities that change as a function of the position. No evident or just quite weak signals could be observed in the high wavenumber part of the spectrum, that is, the characteristic region of hydrogen-heteroelements bonds (-OH, -NH<sub>2</sub>, -NH-C<sub>sp</sub><sup>3</sup>H, -C<sub>sp</sub><sup>2</sup>H, -C<sub>sp</sub>H); however, signals were observable around the 1500–1670  $\text{cm}^{-1}$  region, which is normally associated with the vibrations of the double bond C=C and C=O, particularly the amide group C=O-N-, which normally characterise proteins [35]. Signals between about 1100 and 1000  $\text{cm}^{-1}$  can be generally attributed to weak asymmetric stretching of C-O-C [36]. Some additional signals, originating from CH groups, were observed in two spectral regions (1350–1050  $\text{cm}^{-1}$  and 880–680  $\text{cm}^{-1}$ ) [35].

The internal face (Figure 5B) was less uniform, and there were differences among the areas taken into consideration. The fluorescence was still present, but except for the edges where it was on the contrary very strong (spectrum of zone 15, which has been multiplied by 0.2 to be shown together with the others); this spectral feature was weaker than on the external face (Figure 4A). In this case, it is generally possible to recognise the inorganic mineral present, that is, aragonite or calcite, depending on the position.

As can be expected, the mother-of-pearl area (nacre) was mainly made up of aragonite; however, moving from the edge towards the centre, i.e., from zone 7 towards zone 9, the fluorescence became more intense, and bands that cannot be attributed to calcium carbonate appeared. In particular, in spectrum 9, there was a peak around 1500  $\text{cm}^{-1}$ , which can be associated with organic functional groups, and in addition to other signals with lower wavenumbers also detectable. Bands in this position can be assigned to C=O or to C=C bond vibrations, in agreement with the presence of biomolecules. This trend may have been due to the structure of the nacre and the way in which the animal synthesises it. Nacre is composed of thin hexagonal platelets of aragonite arranged in a continuous parallel manner. Depending on the species, the shape of these tablets changes, but these layers are separated by sheets of organic matrix. Because the way the mollusc grows, near position 7, the nacre was thicker and more continuous so that the platelets formed a compact layer, whereas around position 9, it was thinner, and the new secreted platelets were partially separated. Therefore, the organic matter can be stimulated by the laser. This is particularly evident in position 10, and in subsequent ones, where the shell was macroscopically thinner and the carbonate components more separated. In position 10, traces of organic molecules may also have been due to the adductor muscle attached in that position. The band at about 1500  $\text{cm}^{-1}$  was still present and became stronger and stronger.

All calcium carbonate polymorphs had a sharp peak at about 1080  $\text{cm}^{-1}$  (1085  $\text{cm}^{-1}$  for calcite, 1080  $\text{cm}^{-1}$  for aragonite, 1090  $\text{cm}^{-1}$  for vaterite that also has a secondary weaker peak at 1075  $\text{cm}^{-1}$ ), but in spectra of these positions, they were hidden by a much larger band that also had an evident shoulder at about 1095  $\text{cm}^{-1}$ . A second very intense band was evident at about 1020  $\text{cm}^{-1}$ . In general, it seems that the thinner the shell, the more intense these bands, also because the thickest parts of the shell are those formed first, while the thin ones were secreted by the animal at the end of its growth and can contain many biopolymers. In points close to other extremities, calcite also begins to be present.

Raman spectra were acquired in the shell section (Figure 5C). They were rather similar to each other. In the selected areas, fluorescence was observable, meaning that organic

molecules were present, but generally it was less strong than on the faces, suggesting that the organic components were less abundant inside the shell, and decreased moving from the extremities toward the centre. As one of the main features of these spectra, the band around  $1480\text{ cm}^{-1}$  was present; its relative intensity, however, decreased following the same trend of the fluorescence, being stronger on the extremities.

Inorganic components were more recognisable than on the inner face, and it was possible to discriminate areas where calcite was more abundant (external face and thin end), where aragonite was predominant (internal face thick end), or they coexisted (some central areas). After the complete treatment, the organic part was almost completely gone, as it is possible to observe in Figure 6, which shows Raman spectra collected in several points of the external and inner faces. Raman spectra collected on samples treated for a short period of time show the bands due the organic components. The longer the treatment, the weaker they become.

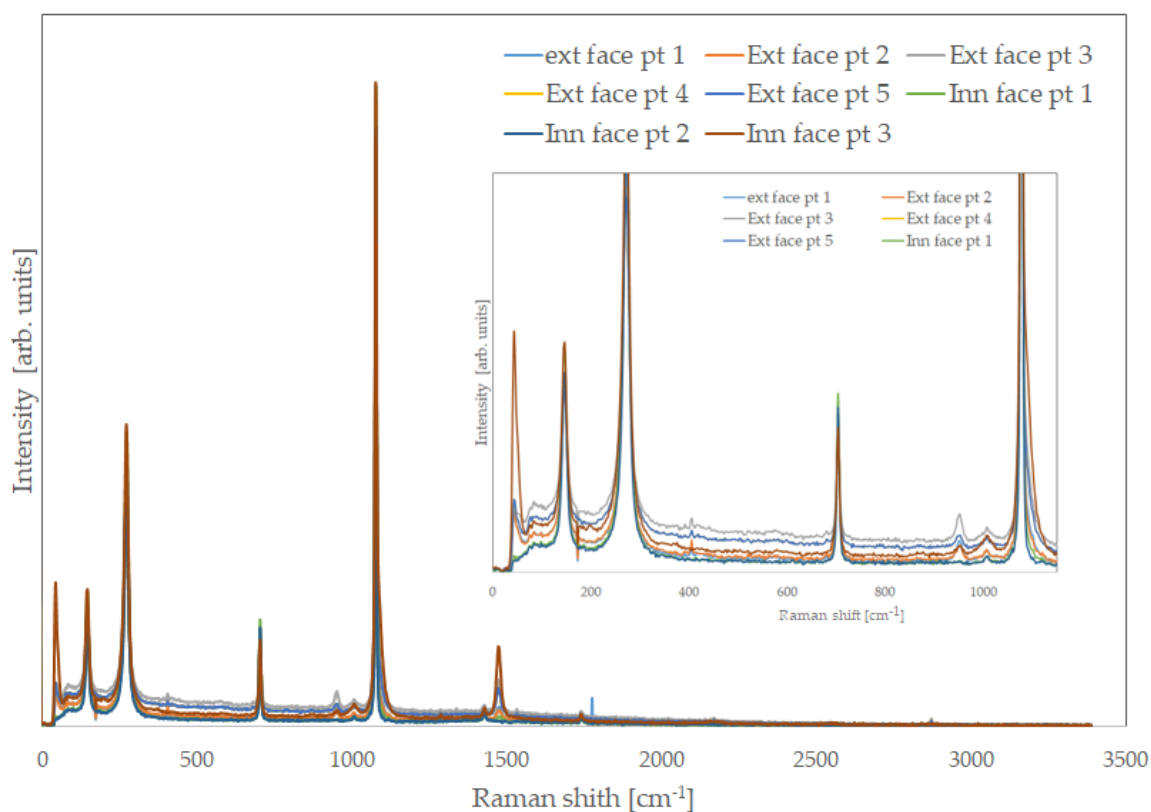


**Figure 6.** Raman spectra of some randomly chosen points on the external and internal face of a shell.

Despite traces of organic components in some places being still present, in general, only peaks of calcium carbonate were recognisable. Table 2 shows the theoretical peak positions of Raman spectra of calcite and aragonite (from [37] and [38], respectively).

In practically all the points where the spectra were acquired, they did not exhibit fluorescence signals, and this finding is in perfect agreement with the complete removal of organic components.

It is very important to note that all the carbonate Raman bands, which were possible to see in the treated specimens, were extremely narrow: for both calcite and aragonite, the most intense peak corresponded to the symmetric stretching of the  $\text{CO}_3$  group, at approximately  $1080\text{ cm}^{-1}$ , and they had a very small FWHM, much narrower than  $5\text{ cm}^{-1}$ . Commercial or synthetic calcium carbonates have values much higher than this. This result indicates the high crystalline grade and confirms the high purity of the carbonate of biogenic origin, in good agreement with the ICP-MS results described previously. Impurities and crystalline defects can indeed induce a broadening and a certain degree of asymmetry in

Raman bands. Large size distribution of crystallites can also have a similar effect. The slow growth of crystals in the shells, mediated by proteins and biopolymers, minimise these effects, and the individual crystals also have a very constant and uniform size.

**Table 2.** Calcite and aragonite Raman peaks.

	Raman Shift (cm <sup>-1</sup> )	
	Calcite [33]	Aragonite [34]
1	155	145
2	282	155
3	713	182
4	1087	192
5	1437	208
6	1749	705
7		716
8		1085
9		1463
10		1576

In the shell section, the spectra were very similar to those observed on the two faces, meaning that the small quantity of organic components, which were found in the untreated specimens, were completely removed. This is an interesting observation, because it suggests that weight loss is not only due to the detachment of periostracum and hypostracum, but also to a real chemical process, and that, thanks to the action of peroxide, water-soluble molecules are released from the shells. It can be imagined, however, that the mechanism of this release is a rather complex path.

The complex proteins secreted by the external epithelial tissue of molluscs, i.e., by the mantle, form the so-called conchiolin. These proteins form a matrix that constitutes the environment in which calcium carbonate crystals nucleate and grow.

There are some methods for extracting the organic component from the shells as these biopolymers are intrinsically attractive, have excellent chemical-physical and mechanical properties, and can have some interesting applications: for example in the biomedical field or even as antibacterials. However, these methods require the mechanical destruction of the shells and the removal of the inorganic part by acid treatments, which are obviously not the aim of the present work, which is instead to keep the shells as little modified as possible.

It is not easy to indicate what the chemical mechanism underlying the process described here is, and further investigations would be required for highlighting this point. Nevertheless, hydrogen peroxide can perturb hydrogen bonds among the macromolecules, causing them to move away from each other [39,40]. Furthermore, it is well known that proteins themselves can degrade under the effect of high concentrations of hydrogen peroxide by action of free radicals, eventually leading to their hydrolysis [41,42].

Polysaccharides behave in a similar manner in respect to H<sub>2</sub>O<sub>2</sub> [43]. Therefore, it can be imagined that hydrogen peroxide can cut biopolymers into smaller units that are more soluble in aqueous environments. In contrast, peroxide has limited or no effect on the inorganic part of the shells. It can therefore be suggested that the main action of the peroxide is to cut away the bonds between the organic layers and the crystalline matrix and possibly to break the large macromolecules into smaller and soluble residues. In part, this also justifies the detachment of the very small sheets of nacre, because the biopolymer chains that are located among them and which help to keep them bound are broken.

Once the organic part has been removed, it is possible to evaluate the ratio between the different polymorphs present overall. For doing this and to evaluate the possible presence of amorphous phases, a sample, after being treated by peroxide, was carefully ground in an agate mortar. The diffraction pattern (XRD) of the obtained powder was acquired (Figure 7); according to these results, it turned out that the valve was made mainly by calcite, about 75%, and the rest was aragonite.

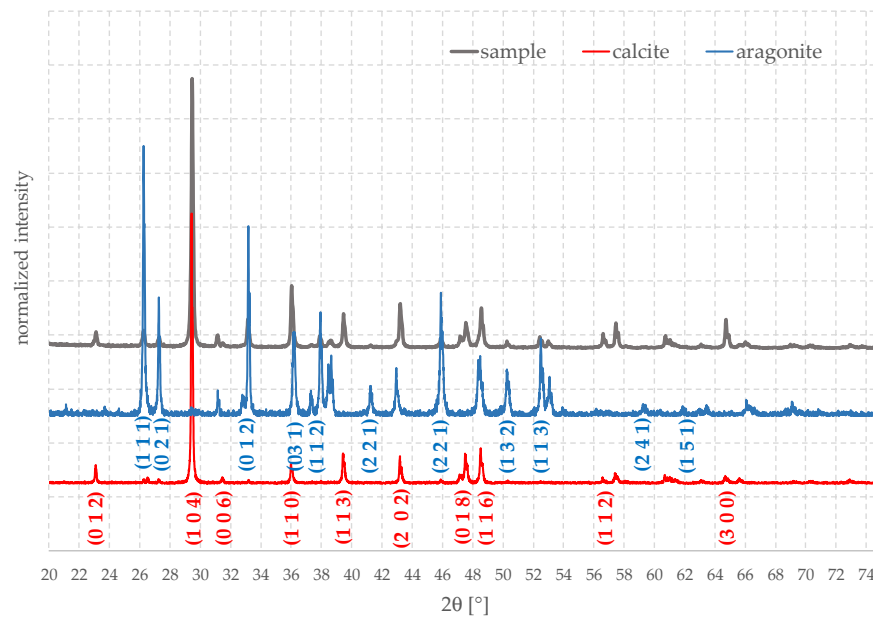


**Figure 7.** XRD analysis of a ground Mytilus shell.

Again, the quality of the material was very high and only calcite, and aragonite were present, without spurious phases, with just some very weak peaks due to  $\text{Na}_2\text{O}$ , that can form during the treatment. All peaks were extremely narrow, indicating the high degree of crystallinity and suggesting that valves are promising raw materials for many possible applications.

The quality of the calcium carbonate resulting from these shells was very high, in terms of purity and crystallinity, especially when compared with commercial materials. This may suggest useful applications as a raw material for industry. It is an absolutely non-toxic product and without any risk for humans and the environment. It should in fact be kept in mind that calcium carbonate is used as a starting material for cements and other construction compounds, being used as an additive in numerous sectors, for example in tires. It is used as a filler in the production of paints, varnishes, paper, rubbers, and glues. Also, it is used in the production of glass and crystals. All these sectors could have many advantages using a better raw starting material. Even the organic layers that detach from the shells could have applications, being rich in interesting biomolecules. They could, for example, have biotechnological applications or be used to produce biocompatible and environmentally friendly polymers and hydrogels.

This treatment also allows us to better analyse the microstructure of the valves, as it can also be easily seen in SEM images shown in Figure 8A–H.

The structure of the shells of bivalves and molluscs in general has been thoroughly investigated, and there are numerous scientific articles and reviews on the subject [12,44–46].

The external face (Figure 8A,B) but also for a certain degree the internal one of an untreated sample do not show characteristic details, because they are covered by very homogeneous layers. The section, however, is much more organised and the different microstructures are clearly evident. But, also for it, the treatment with hydrogen peroxide has a positive effect, and the characteristics are well highlighted. Sometimes, the microstructure was highlighted by more vigorous attacks than the milder treatment described in this work. Therefore, it may be imagined that it is less altered for observations.

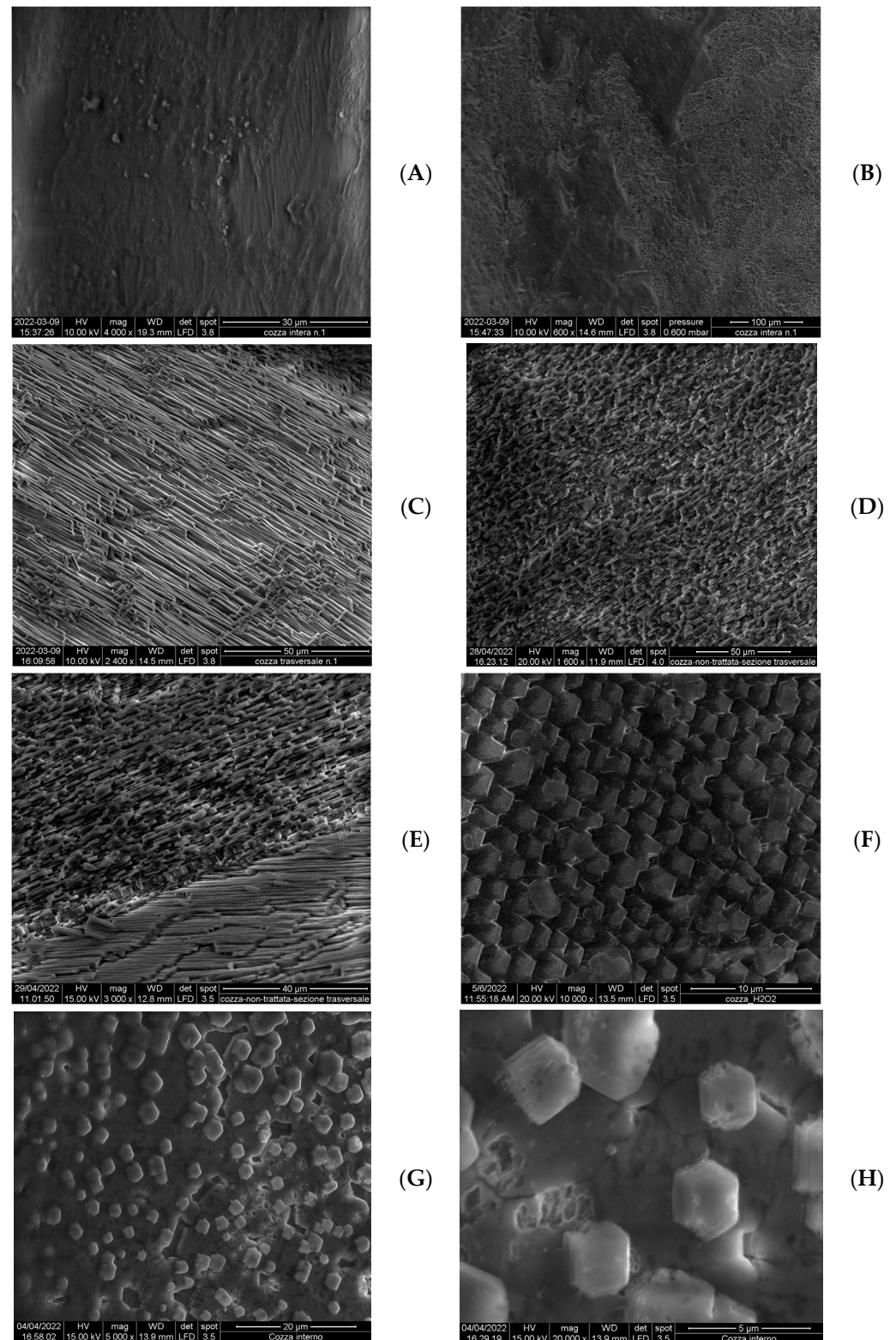


**Figure 8.** SEM micrographs of different areas of a *Mytilus* shell before and after the treatment with hydrogen peroxide. (A,B): external face of an untreated specimen; (C,D): images of the section of a shell specimen; (E): boundary between prismatic part and nacreous layer; (F–H): nacreous layer showing the hexagonal crystals.

The inner part of a shell is formed by prismatic crystal, as can be seen in Figure 8C,D, which shows the section of a treated shell. A very clear separation from the nacreous layer exists (Figure 8E).

Nacre, in itself, is composed of hexagonal platelets, arranged in a parallel manner, as can be easily seen in Figure 8F–H. These platelets have a very uniform size, just a few microns large. Depending on the position in the valve, they are more or less compact. This is due to the moment in which they were formed. In the most recent part of growing shell, these crystallites are separated and isolated. Furthermore, it can be observed that they grow preferentially at the joints between the grain boundaries of the underlying layer, which is much more compact. The size of these isolated crystallites is also roughly constant, and this strongly suggests that they begin forming at the same time. Indeed, even if the growth of the shell occurs in successive layers, each layer is formed when the one below is not completely compact.

#### 4. Conclusions

This work presents a discussion about the use of concentrated hydrogen peroxide solution for removing and separating the organic components from the inorganic part in mollusc shells. Shells are an intriguing example of a composite material. In life, the animal produces calcium carbonate microcrystals in the form of various polymorphs, such calcite and aragonite, thanks to the action of specialised proteins and biopolymers, based on its functional needs.

The process of removal of the inorganic part and recover of organic molecules, which can successively have various applications, is relatively easy to perform using acid baths. The opposite process is more difficult.

A bath of a few hours in concentrated hot hydrogen peroxide completely removes the organic component from the valves without altering the inorganic structure.

The method discussed here is very effective, has a low cost, and is environmentally friendly because no pollutant and expansive reagents are required. Raman, XRD, and morphological analyses showed the excellent crystallographic quality of the calcium carbonate crystals that make up the shells, and ICP-MS instead showed their very high chemical purity.

This makes the shells extremely interesting starting raw materials for applications in the building field, especially with a view of limiting greenhouse gas emissions and CO<sub>2</sub>, as well as being more environmentally sustainable.

A possible future development could be represented by the optimisation of the hydrogen peroxide concentration, the process temperature, and the time necessary to obtain the removal of the organic components. Furthermore, it could be systematically applied to other mollusc species.

**Author Contributions:** Conceptualisation, A.U.; methodology, A.U., F.C., N.F., G.M., A.G., S.S. and S.B.; validation, S.B. and A.R.; investigation, A.U., F.C., N.F., G.M., A.G., S.S. and S.B.; writing—original draft preparation, A.U.; writing—review and editing, S.C., C.T., N.F. and A.U. All authors have read and agreed to the published version of the manuscript.

**Funding:** This research received no external funding.

**Data Availability Statement:** The original contributions presented in this study are included in the article; further inquiries can be directed to the corresponding author.

**Conflicts of Interest:** The authors declare no conflicts of interest.

#### References

1. Omelon, S.; Georgiou, J.; Henneman, Z.J.; Wise, L.M.; Sukhu, B.; Hunt, T.; Wynnyckyj, C.; Holmyard, D.; Bielecki, R.; Grynpas, M.D. Control of vertebrate skeletal mineralization by polyphosphates. *PLoS ONE* **2009**, *4*, e5634. [[CrossRef](#)] [[PubMed](#)]
2. Huang, J.; Zhang, R. The Mineralization of Molluscan Shells: Some Unsolved Problems and Special Considerations. *Front. Mar. Sci.* **2022**, *9*, 874534. [[CrossRef](#)]
3. Simonet Roda, M.; Griesshaber, E.; Ziegler, A.; Rupp, U.; Yin, X.; Henkel, D.; Häussermann, V.; Laudien, J.; Brand, U.; Eisenhauer, A.; et al. Calcite fibre formation in modern brachiopod shells. *Sci. Rep.* **2019**, *9*, 598. [[CrossRef](#)] [[PubMed](#)]
4. Zaquin, T.; Pinkas, I.; Di Bisceglie, A.P.; Mucaria, A.; Milita, S.; Fermani, S.; Goffredo, S.; Mass, T.; Falini, G. Exploring Coral Calcification by Calcium Carbonate Overgrowth Experiments. *Crystal. Growth Des.* **2022**, *22*, 5045–5053. [[CrossRef](#)]

5. Sardo, A.; Orefice, I.; Balzano, S.; Barra, L.; Romano, G. Mini-Review: Potential of Diatom-Derived Silica for Biomedical Applications. *Appl. Sci.* **2021**, *11*, 4533. [CrossRef]
6. Lazarus, D.B.; Kotrc, B.; Wulf, G.; Schmidt, D.N. Radiolarians decreased silicification as an evolutionary response to reduced Cenozoic ocean silica availability. *Proc. Natl. Acad. Sci. USA* **2009**, *106*, 9333–9338. [CrossRef]
7. Somu, D.R.; Cracchiolo, T.; Longo, E.; Greving, I.; Merk, V. On stars and spikes: Resolving the skeletal morphology of planktonic Acantharia using synchrotron X-ray nanotomography and deep learning image segmentation. *Acta Biomater.* **2023**, *159*, 74–82. [CrossRef]
8. Łukowiak, M. Utilizing sponge spicules in taxonomic, ecological and environmental reconstructions: A review. *PeerJ* **2020**, *8*, e10601. [CrossRef] [PubMed] [PubMed Central]
9. Wiltschko, R.; Wiltschko, W. The magnetite-based receptors in the beak of birds and their role in avian navigation. *J. Comp. Physiol. A Neuroethol. Sens. Neural. Behav. Physiol.* **2013**, *199*, 89–98. [CrossRef] [PubMed] [PubMed Central]
10. Schofield, R.M.S.; Bailey, J.; Coon, J.J.; Devaraj, A.; Garrett, R.W.; Goggans, M.S.; Hebnner, M.G.; Lee, B.S.; Lee, D.; Lovern, N.; et al. The homogenous alternative to biomineralization: Zn- and Mn-rich materials enable sharp organismal tools that reduce force requirements. *Sci. Rep.* **2021**, *11*, 17481. [CrossRef]
11. Hillerton, J.E.; Vincent, J.F.V. The Specific Location of Zinc in Insect Mandibles. *J. Exp. Biol.* **1982**, *10*, 333–336. [CrossRef]
12. Louis, V.; Besseau, L.; Lartaud, F. Step in Time: Biomineralisation of Bivalve's Shell. *Front. Mar. Sci.* **2022**, *9*, 906085. [CrossRef]
13. Okada, S.; Chen, C.; Watsuji, T.; Nishizawa, M.; Suzuki, Y.; Sano, Y.; Bissessur, D.; Deguchi, S.; Takai, K. The making of natural iron sulfide nanoparticles in a hot vent snail. *Proc. Natl. Acad. Sci. USA* **2019**, *116*, 20376–20381. [CrossRef] [PubMed]
14. Oertle, A.; Szabó, K. Thermal Influences on Shells: An Archaeological Experiment from the Tropical Indo-pacific. *J. Archaeol. Method Theory* **2023**, *30*, 536–564. [CrossRef]
15. Yoshioka, S.; Kitano, Y. Transformation of aragonite to calcite through heating. *Geochem. J.* **1985**, *19*, 245–249. [CrossRef]
16. Boettcher, A.L.; Wyllie, P.J. The Calcite-Aragonite Transition Measured in the System CaO-CO<sub>2</sub>-H<sub>2</sub>O. *J. Geol.* **1968**, *76*, 214–330. [CrossRef]
17. Nudelmann, F.; Gotliv, B.A.; Addadi, L.; Steve, W. Mollusk shell formation: Mapping the distribution of organic matrix components underlying a single aragonitic tablet in nacre. *J. Struct. Biol.* **2006**, *153*, 176–187. [CrossRef] [PubMed]
18. Jackson, A.P.; Vincent JF, V.; Turner, R.M. The mechanical design of nacre. *Proc. R. Soc. B Biol. Sci.* **1988**, *234*, 415–440. [CrossRef]
19. Radhaa, A.V.; Forbesa, T.Z.; Killianb, C.E.; Gilbert PU, P.A.; Navrotsky, A. Transformation and crystallization energetics of synthetic and biogenic amorphous calcium carbonate. *Proc. Natl. Acad. Sci. USA* **2010**, *107*, 16438–16443. [CrossRef] [PubMed]
20. Sawada, N.; Toyohara, H.; Nakano, T. A New Cleaning Method for Accurate Examination of Freshwater Gastropod Shell Specimens Covered with Iron-rich Deposits. *Species Divers.* **2021**, *26*, 217–224. [CrossRef]
21. Kaya, M.; Baran, T.; Karaarslan, M. A new method for fast chitin extraction from shells of crab, crayfish and shrimp. *Nat. Prod. Res.* **2015**, *29*, 1477–1480. [CrossRef] [PubMed]
22. Falster, G.; Delean, S.; Tyler, J. Hydrogen peroxide treatment of natural lake sediment prior to carbon and oxygen stable isotope analysis of calcium carbonate. *Geochem. Geophys. Geosyst.* **2018**, *19*, 3583–3595. [CrossRef]
23. Smith, A.M.; Key Jr, M.M.; Henderson, Z.E.; Davis, V.C.; Winter, D.J. Pretreatment for removal of organic material is not necessary for X-ray-diffraction determination of mineralogy in temperate skeletal carbonate. *J. Sediment. Res.* **2016**, *86*, 1425–1433. [CrossRef]
24. Hou, Y.; Shavandi, A.; Carne, A.; Bekhit, A.A.; Ng, T.B.; Cheung, R.C.F.; Bekhit, A.E.D.A. Marine shells: Potential opportunities for extraction of functional and health-promoting materials. *Crit. Rev. Environ. Sci. Technol.* **2016**, *46*, 1047–1116. [CrossRef]
25. Lertvachirapaiboon, C.; Parnklang, T.; Pienpinijtham, P.; Wongravee, K.; Thammacharoen, C.; Ekgasit, S. Selective colors reflection from stratified aragonite calcium carbonate plates of mollusk shells. *J. Struct. Biol.* **2015**, *191*, 184–189. [CrossRef]
26. Available online: <https://www.molluscabase.org/aphia.php?p=taxdetails&id=397041> (accessed on 10 May 2024).
27. Available online: <https://www.iso.org/standard/53394.html> (accessed on 10 May 2024).
28. Giribet, G. Bivalvia. In *Phylogeny and Evolution of the Mollusca*; University of California Press: Berkeley, CA, USA, 2008. [CrossRef]
29. Harris, M.G.; Torres, J.; Tracewell, L. pH and H<sub>2</sub>O<sub>2</sub> concentration of hydrogen peroxide disinfection Systems. *Optom. Vis. Sci.* **1988**, *65*, 527–535. [CrossRef]
30. Strehse, J.S.; Maser, E. Marine bivalves as bioindicators for environmental pollutants with focus on dumped munitions in the sea: A review. *Mar. Environ. Res.* **2020**, *158*, 105006. [CrossRef] [PubMed]
31. Al-Awadi, M.; Clark, W.J.; Moore, W.R.; Herron, M.; Zhang, T.; Zhao, W.; Hurley, N.; Kho, D.; Montaron, B.; Sadooni, F. Dolomite: Perspectives on a perplexing mineral. *Oilfield Rev.* **2009**, *21*, 32–45.
32. Antao, S.; Hassan, I.; Mulder, M.; Lee, P.L.; Toby, B.H. In situ study of the R3c → R3m orientational disorder in calcite. *Phys. Chem. Miner.* **2009**, *36*, 159–169. [CrossRef]
33. Ulian, G.; Valdrè, G. The effect of long-range interactions on the infrared and Raman spectra of aragonite (CaCO<sub>3</sub>, Pmcn) up to 25 GPa. *Sci. Rep.* **2023**, *13*, 2725. [CrossRef]
34. Christy, A.G. A Review of the Structures of Vaterite: The Impossible, the Possible, and the Likely. *Cryst. Growth Des.* **2017**, *17*, 3567–3578. [CrossRef]
35. Kuhar, N.; Sil, S.; Umamathy, S. Potential of Raman spectroscopic techniques to study proteins. *Spectrochim. Acta Part A Mol. Biomol. Spectrosc.* **2021**, *258*, 119712. [CrossRef] [PubMed]
36. Ettah, I.; Lorna Ashton, L. Engaging with Raman Spectroscopy to Investigate Antibody Aggregation. *Antibodies* **2018**, *7*, 24. [CrossRef]

37. King, H.E.; Geisler, T. Tracing Mineral Reactions Using Confocal Raman Spectroscopy. *Minerals* **2018**, *8*, 158. [[CrossRef](#)]
38. Tomić, Z.P.; Petre Makreski, P.; Gajic, B. Identification and spectra–structure determination of soil minerals: Raman study supported by IR spectroscopy and X-ray powder diffraction. *J. Raman Spectrosc.* **2010**, *41*, 582–586. [[CrossRef](#)]
39. Parida, C.; Chowdhuri, S. Effects of Hydrogen Peroxide on the Hydrogen Bonding Structure and Dynamics of Water and Its Influence on the Aqueous Solvation of the Insulin Monomer. *J. Phys. Chem. B* **2023**, *127*, 10814–10823. [[CrossRef](#)]
40. Le, H.-T.; Chaffotte, A.F.; Demey-Thomas, E.; Vinh, J.; Friguier, B.; Mary, J. Impact of Hydrogen Peroxide on the Activity, Structure, and Conformational Stability of the Oxidized Protein Repair Enzyme Methionine Sulfoxide Reductase A. *J. Mol. Biol.* **2009**, *393*, 58–66. [[CrossRef](#)]
41. Fligel, S.E.; Lee, E.C.; McCoy, J.P.; Johnson, K.J.; Varani, J. Protein degradation following treatment with hydrogen peroxide. *Am. J. Pathol.* **1984**, *115*, 418–425.
42. Song, I.-K.; Lee, J.-J.; Cho, J.-H.; Jeong, J.; Shin, D.-H.; Lee, K.-J. Degradation of Redox-Sensitive Proteins including Peroxiredoxins and DJ-1 is Promoted by Oxidation-induced Conformational Changes and Ubiquitination. *Sci. Rep.* **2016**, *6*, 34432. [[CrossRef](#)] [[PubMed](#)]
43. Chen, X.; Sun-Waterhouse, D.; Yao, W.; Li, X.; Zhao, M.; You, L. Free radical-mediated degradation of polysaccharides: Mechanism of free radical formation and degradation, influence factors and product properties. *Food Chem.* **2021**, *365*, 130524. [[CrossRef](#)] [[PubMed](#)]
44. Checa, A.G. Physical and Biological Determinants of the Fabrication of Molluscan Shell Microstructures. *Front. Mar. Sci.* **2018**, *5*, 353. [[CrossRef](#)]
45. Kempf, H.L.; Gold, D.A.; Carlson, S.J. Investigating the Relationship between Growth Rate, Shell Morphology, and Trace Element Composition of the Pacific Littleneck Clam (*Leukoma staminea*): Implications for Paleoclimate Reconstructions. *Minerals* **2023**, *13*, 814. [[CrossRef](#)]
46. Duarte, C.M.; Rodriguez-Navarro, A.B.; Delgado-Huertas, A.; Krause-Jensen, D. Dense *Mytilus* Beds Along Freshwater-Influenced Greenland Shores: Resistance to Corrosive Waters Under High Food Supply. *Estuaries Coasts* **2020**, *43*, 387–395. [[CrossRef](#)]

**Disclaimer/Publisher’s Note:** The statements, opinions and data contained in all publications are solely those of the individual author(s) and contributor(s) and not of MDPI and/or the editor(s). MDPI and/or the editor(s) disclaim responsibility for any injury to people or property resulting from any ideas, methods, instructions or products referred to in the content.